

Transfer-Free Integration of Graphene on Suspended Micro-Hotplates for No2 Sensing

Sacco, Leandro N.; Vollebregt, Sten

DOI

[10.1109/MEMS61431.2025.10917898](https://doi.org/10.1109/MEMS61431.2025.10917898)

Publication date

2025

Document Version

Final published version

Published in

2025 IEEE 38th International Conference on Micro Electro Mechanical Systems, MEMS 2025

Citation (APA)

Sacco, L. N., & Vollebregt, S. (2025). Transfer-Free Integration of Graphene on Suspended Micro-Hotplates for No2 Sensing. In *2025 IEEE 38th International Conference on Micro Electro Mechanical Systems, MEMS 2025* (pp. 904-907). (Proceedings of the IEEE International Conference on Micro Electro Mechanical Systems (MEMS)). IEEE. <https://doi.org/10.1109/MEMS61431.2025.10917898>

Important note

To cite this publication, please use the final published version (if applicable).
Please check the document version above.

Copyright

Other than for strictly personal use, it is not permitted to download, forward or distribute the text or part of it, without the consent of the author(s) and/or copyright holder(s), unless the work is under an open content license such as Creative Commons.

Takedown policy

Please contact us and provide details if you believe this document breaches copyrights.
We will remove access to the work immediately and investigate your claim.

Green Open Access added to TU Delft Institutional Repository

'You share, we take care!' - Taverne project

<https://www.openaccess.nl/en/you-share-we-take-care>

Otherwise as indicated in the copyright section: the publisher is the copyright holder of this work and the author uses the Dutch legislation to make this work public.

TRANSFER-FREE INTEGRATION OF GRAPHENE ON SUSPENDED MICRO-HOTPLATES FOR NO₂ SENSING

Leandro N. Sacco, and Sten Vollebregt

Laboratory of Electronic Components, Technology and Materials (ECTM), Microelectronics Department, Delft University of Technology, THE NETHERLANDS

ABSTRACT

In this work, we demonstrate the use of a micro-hotplate (MHP) with graphene integrated without transfer step for NO₂ sensing. The MHP can rapidly recover the device to its initial conditions by applying a brief heat pulse. Moreover, by employing a process without graphene transfer, we prevent random polymer contamination from the transfer process. The (up to 8) graphene sensors on a single MHP show a very similar response. Finally, we demonstrate that we can extract the relative humidity from the device's response immediately after the MHP is turned off in a humid environment.

KEYWORDS

Gas sensors, graphene, micro hotplate, humidity

INTRODUCTION

Graphene has sparked tremendous interest for application in gas sensors because of its large specific surface area, chemical stability, and the possibility of functionalizing the graphene to improve selectivity [1]. Moreover, graphene gas sensors can provide good sensitivity at low or even room temperature [2], which can reduce power consumption that hampers the mobile application of commercially available gas sensors based on metal oxides.

However, several challenges remain. One of these is the slow recovery of graphene at room temperature, requiring external stimuli such as heat or UV to accelerate desorption [3]. The 2nd issue is the sample-to-sample variation of graphene gas sensors due to random polymer contamination from the transfer step [4]. Random variations will make it challenging to study functionalization approaches aimed at improving selectivity, as these fluctuations could be in the same order as the functionalization effect.

Here, we resolved both issues by fabricating a suspended MHP on which we integrate up to 8 multi-layer graphene gas sensor strips without requiring transfer. We achieve this by combining a Si micromachining MHP process with a Mo-catalyst-based transfer-free graphene approach [5, 6]. Another layer of Mo is used as heater material, which can withstand the high temperature of the graphene deposition. The MHP allows for rapid recovery by applying short heat pulses, keeping the overall power consumption relatively low (mW range). By integrating the graphene on top of the MHP using a transfer-free approach, we mitigate the random polymer contamination associated with the transfer step. It also prevents adhesion issues when transferring and patterning graphene on the SiN_x-encapsulated heaters [7]. The devices were successfully realized on 100 mm wafers, and tested towards NO₂ and at different relative humidities.

EXPERIMENTAL

Device fabrication

The fabrication process for realizing the Mo-based micro-hotplates with transfer-free multi-layer graphene is shown in Fig. 1. A single-sided polished 100 mm Si (100) wafer with a thickness of 525 μ m was used as substrate.

First, the wafers are thermally oxidized to obtain 500 nm SiO₂, followed by 500 nm of low-stress LPCVD SiN_x (Fig. 1a). For the micro-heater, a 200 nm thick Mo layers was sputtered and immediately covered by a 350 nm PECVD SiO₂ layer that functions as a hard mask. Both layers were patterned using photolithography employing an i-line waferstepper, followed by RIE etching in, subsequently, fluor and chlorine chemistry (Fig. 1b). After this the PECVD oxide was etched in BHF (1:7). Next, another 350 nm of PECVD SiO₂ was deposited, and finally the whole heater was encapsulated by 250 nm low-stress LPCVD SiN_x (Fig. 1c).

On the backside of the wafer a 6 μ m thick PECVD oxide was deposited as hard mask, and patterned together with the LPCVD SiN_x using fluor-based RIE (Fig. 1d). This is followed by the sputter deposition of 50 nm Mo that will act as catalyst for the CVD graphene growth. This layer is subsequently patterned using photolithography and Cl-based RIE. After this, openings were etched in the top SiN_x using another lithography step followed by fluor RIE,

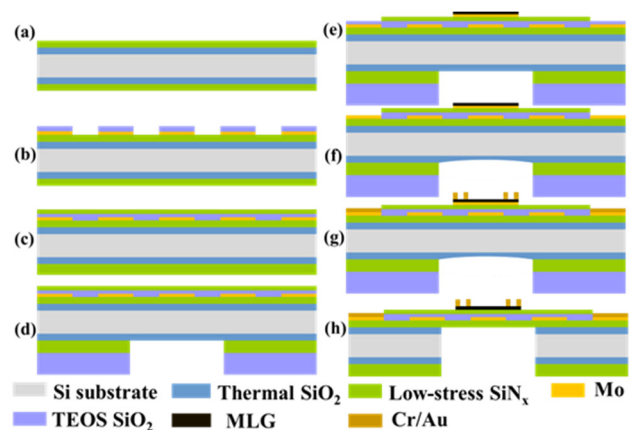


Figure 1: Process flow for the fabrication of the micro-hotplate with integrated multi-layered graphene chemistors: a) deposition of thermal SiO₂ and LPCVD SiN_x; b) deposition and patterning of the Mo-heater with a PECVD SiO₂ hard mask; c) encapsulation of the heater with PECVD SiO₂ and LPCVD SiN_x; d) backside deposition and etching of PECVD oxide hard mask for DRIE; e) deposition of Mo catalyst, partial opening of the heater contacts and CVD deposition of graphene; f) wet etching of the remaining oxide in the heater contacts; g) patterning of Cr/Au contact to the heater and graphene using lift-off; h) DRIE of the Si wafer to suspend the heater and removal of the Mo catalyst using wet etching.

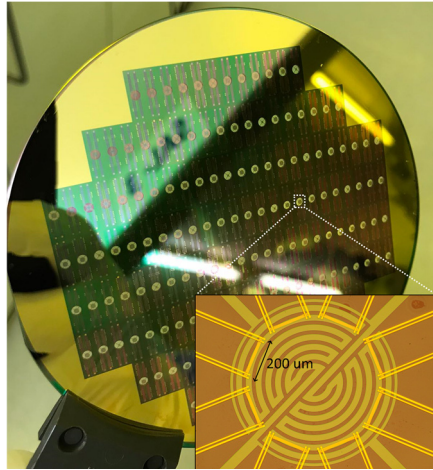


Figure 2: Photograph of a 100 mm wafer showcasing 156 suspended micro-hotplates with integrated graphene strips. Inset: microphotograph of a suspended MHP with eight graphene strips with each 4 electrical contacts. The area between the inner two contacts is 200x20 μm (LxW). which will later be used to contact the heater.

The multi-layered graphene was grown using an AIXTRON Blackmagic Pro at 935 $^{\circ}\text{C}$ using $\text{Ar}/\text{H}_2/\text{CH}_4$ (960/40/25 sccm) at 25 mbar (Fig. 1e). Next, the remaining SiO_2 in the heater contact openings is removed using BHF (1:7), Fig. 1f. During graphene growth the Mo heater has to be fully encapsulated to prevent graphene nucleation on the heater. After this, a negative resist was coated and exposed, followed by Cr/Au (10/100 nm) e-beam evaporation and lift-off in NMP at 70 $^{\circ}\text{C}$ (Fig. 1g). This metal layer acts as a contact to the graphene chemristors and Mo heaters.

To finalize the device fabrication, the SiN_x membranes encapsulating the heater are suspended by removing the Si from the backside using DRIE (Fig. 2). After this, a photoresist layer was applied, and the wafers were diced. Next, the resist was removed in acetone, and the Mo catalyst was gently etched using H_2O_2 (31 %) following the transfer-free approach [5] (Fig. 1h). To test the samples in the gas sensing setup, the dies were wire-bonded to ceramic PCBs.

Material analysis and device testing

Raman spectroscopy was performed using a Renishaw inVia with 633 nm HeNe laser to analyze the graphene. To characterize the MHP, an Infratec VarioCAM HD with 0.5x close-up lens was used.

The gas sensing tests were performed in a stainless-steel chamber. The gases were generated using an Owlstone V-OVG with NO_2 permeation tube and 99.999% N_2 as carrier gas. To control the humidity, an OHG-4 was used with DI water. The relative humidity in the chamber was measured using an Omni Sensors OHT20T, which is inserted at the side of the test chamber. Gases were inserted directly above the sample using a small showerhead.

A two-channel Keithley 2612B SMU was used for 4-point electrical measurements and to control the MHP. Time multiplexing was used to measure the different devices on a single MHP, using an Agilent 34970A with a 34901A multiplexer module. A LabVIEW script was developed to read out the sensors and control the MHP. The

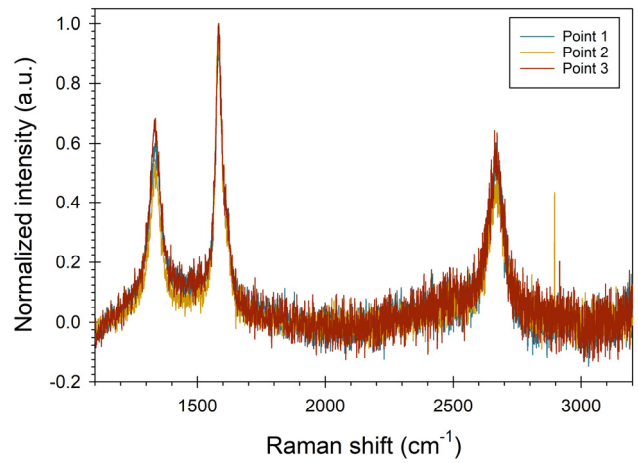


Figure 3: Raman data obtained from different points of a graphene strip after Mo catalyst removal. The spectrum is normalized to the G peak at 1580 cm^{-1} .

graphene devices were biased with 1V, and the micro-heater was biased with 1.5V when turned on to reach a temperature of 140 $^{\circ}\text{C}$.

RESULTS AND DISCUSSION

The presence of graphene was confirmed using Raman spectroscopy, which was obtained from 3 points taken from a graphene strip after Mo catalyst removal (Fig. 3). Due to the suspended membrane, the signal from the graphene is relatively weak, resulting in a low signal-to-noise ratio. From the spectrum, it can be concluded that multi-layered turbostratic graphene is present due to the I_{2D}/I_G being smaller than 1, which can furthermore be fitted by a single Lorentzian [8]. The graphene is relatively defective, with an average I_D/I_G ratio of 0.54. This is more defective than previous devices realized without MHP [5], possibly due to the extensive post-processing of the device after graphene CVD.

Several 1 mm diameter heaters were calibrated using an IR camera while changing the bias [6]. The average measured temperature from the heater vs. the total applied power is shown in Fig. 4. As can be observed, the measured heaters

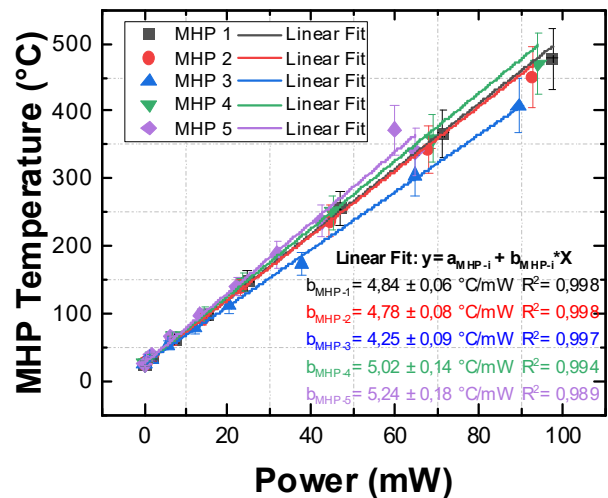


Figure 4: Average temperature of the suspended heater as measured by an IR camera as a function of the applied power. The different responses were linearly fitted as indicated by the values in the figure.

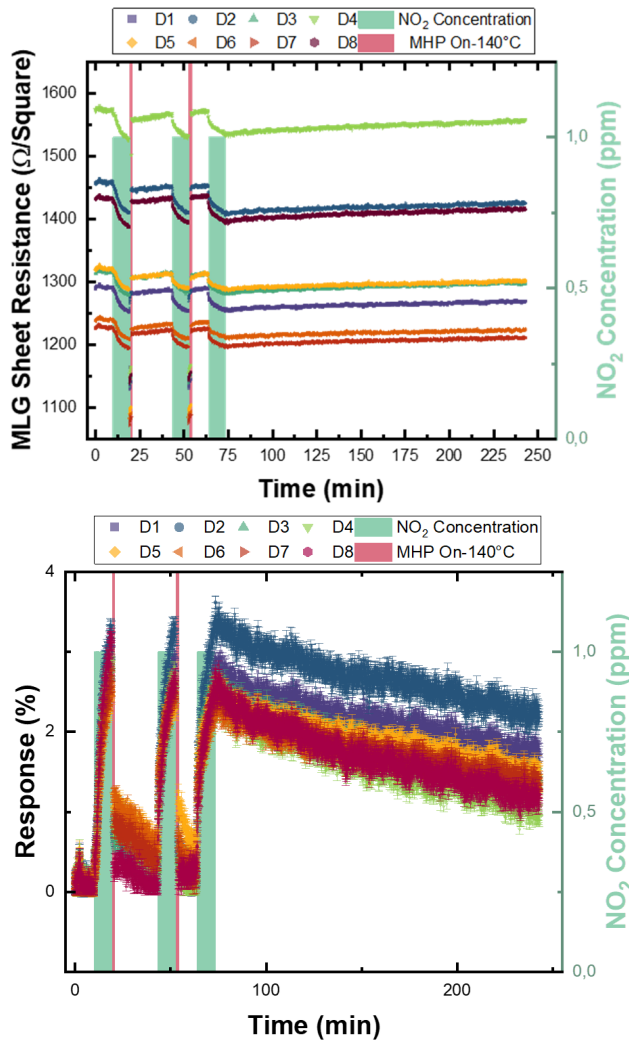


Figure 5: Top figure: response of eight time-multiplexed graphene strips to three 10 min long pulses of 1 ppm NO₂. After the first two pulses, a 90 second heating period was applied with a target temperature of 140 °C. During the whole experiment N₂ is flowing in the chamber. Bottom figure: change of resistance normalized with respect to the resistance just before the first pulse for the same dataset.

show a linear response with only slight variations between the heaters at temperatures below 200°C. On average, the heater response is 3.38 mW/°C, where a_{MHP} is room temperature. At ~34 mW the heaters reach 140 °C. The power consumption of the heaters was not optimized and could be reduced by improving the thermal design and the materials used, as SiN_x has a relatively high thermal conductivity.

A sensor chip with 8 graphene devices was measured using time multiplexing by exposing the device to three 10-minute-long pulses of 1 ppm of NO₂ in an N₂ carrier gas. After the first two pulses, the heater was turned on to reach 140 °C for 90 seconds. The measured resistances are shown in Fig. 5(top).

Upon exposure to NO₂, the resistance of graphene decreases (current increases under constant voltage bias), which is typical for p-type doped graphene as NO₂ acts as an acceptor [2]. When heated, the resistance further decreases due to the negative temperature coefficient of

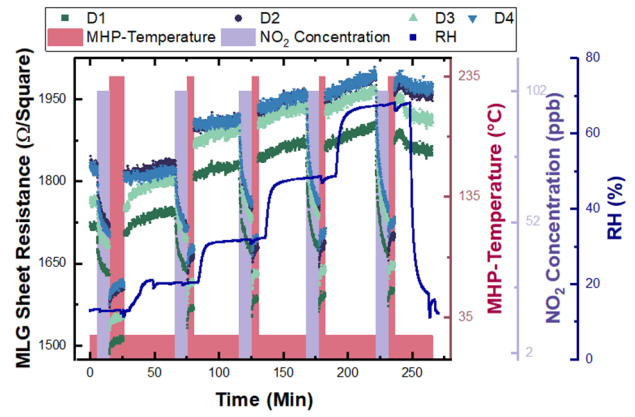


Figure 6: Measured resistances of 4 graphene strips on a single MHP as response to 102 ppb of NO₂ at different humidities. The MHP is powered to 235 °C after the NO₂ supply is stopped. Between the NO₂ pulses the relative humidity is changed from 10% to 70% (dark blue line).

resistance for the multi-layered graphene used in this study [9]. The different strips on the same heater display some variations in their resistance, which we suspect originates from process variations, especially at the end of the process where the Mo catalyst is wet etched on die-level.

In Fig. 5(bottom) the resistance change calculated by Eq. 1 is shown, where R_0 is the average resistance taken from 30 seconds of measurements before the first NO₂ pulse, and R the resistance at the specific timestamp:

$$Response = \frac{R_0 - R}{R_0} [\%] \quad (1)$$

As can be seen, the response to the gas of the eight different sensors is similar, irrespective of their base resistance. This underlines the potential of this approach to realizing graphene gas sensors with small variations. The data points when the heater is enabled have been removed for clarity. After each NO₂ pulse, the average response is $2.83 \pm 0.26\%$, $2.64 \pm 0.30\%$, and $2.51 \pm 0.32\%$, respectively. From the figure, it becomes clear that the heat pulse almost completely recovers the device back to R_0 , while without it, the slow recovery typical for graphene is observed. Even after 1.5 hours of exposure to just N₂, the device does not fully recover without the heat pulse.

Another chip with 4 graphene strips with the same dimensions integrated on one micro hotplate has been tested to 102 ppb of NO₂ at different relative humidities (RH). After each NO₂ exposure, a heat pulse of approximately 235 °C is applied. Before the next NO₂ exposure, the RH is changed from 10% to 70% in steps of 10-15%. The measured resistance of the 4 devices during the experiment is shown in Fig. 6.

The response to each fixed concentration NO₂ pulse increases with increasing humidity, as is also shown in Fig. 7. The presence of water enhances the response to NO₂ significantly due to an increase in charge transfer by water dipole screening [10].

In contrast to our previous work [6], the device does not show a strong response to changes in RH in the timeframe between the heat pulse and subsequent NO₂ exposure. We postulate that this is due to the difference in experimental procedure. In the previous experiment, dry N₂

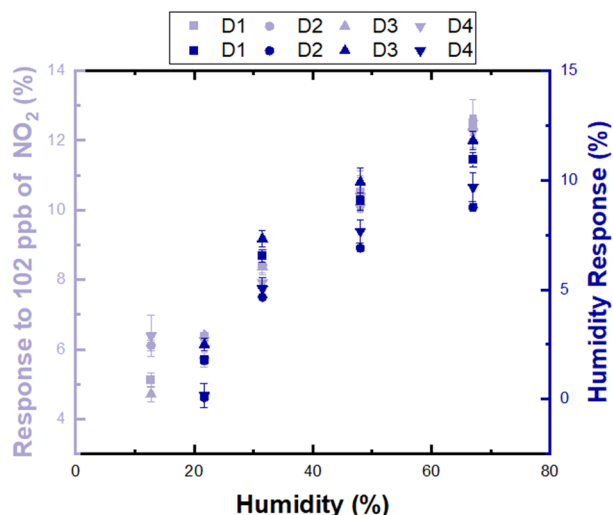


Figure 7: Calculated response of the four graphene to 102 ppb of NO₂ at different RH (left y-axis). The right y-axis shows the calculated response to humidity obtained after the MHP is turned-off.

was flown over the sensors before a different RH exposure was introduced in the chamber [6]. In contrast, here, a specific concentration of water is always present. We assume that the water reabsorbs immediately on the graphene when the MHP is turned off. Due to this, most absorption sites on the graphene are already occupied when the RH changes, resulting in only a small change in the resistance.

This assumption is further confirmed by comparing the resistance after turning off the heater to the average resistance at 10% RH. We calculated this humidity response using Eq. (1), where R_0 is now the resistance at 10% RH (Fig. 7, right y-axis). The obtained response is close to the previously calculated sensitivity to RH [6], although a direct comparison cannot be made as in the previous work for R_0 , the resistance in dry air was used. Further experiments, including a period of exposure to dry N₂ should be performed to obtain the sensitivity to RH.

CONCLUSION

We have demonstrated an approach for fabricating up to 8 multi-layered graphene strips without a transfer step directly on a micro hotplate. The presence of graphene was confirmed using Raman spectroscopy. Furthermore, the temperature response of the MHP was characterized.

While the devices show some base resistance variations, their response to NO₂ is relatively similar. In a dry environment, the response to 1 ppm NO₂ is $2.83 \pm 0.26\%$. When exposed to NO₂ in a humid environment, a much larger response is obtained, up to $\sim 12\%$ for 102 ppb NO₂ at an RH of 70%. This enhanced sensing behaviour has previously been observed in the literature.

Finally, while the devices show little immediate change when changing the RH, we have demonstrated that it could be possible to extract the RH from the resistance difference between that at low humidity and directly after switching off the MHP. This work shows the potential of this platform for further studying graphene for gas sensing applications.

ACKNOWLEDGEMENTS

The authors would like to thank the Else Kooi Laboratory staff for supporting manufacturing the devices and Mudassir Husain for obtaining the Raman spectra. Part of this research has received funding as part of the AGRARSENSE project from the Chips Joint Undertaking (JU) under Grant Agreement No. 101095835. The JU receives support from the European Union's Horizon Europe research and innovation programme and Sweden, Czechia, Finland, Ireland, Italy, Latvia, Netherlands, Poland, Spain, Norway, Türkiye.

REFERENCES

- [1] Z. Chen, J. Wang, and Y. Wang, "Strategies for the performance enhancement of graphene-based gas sensors: A review", *Talanta*, vol. 235, p. 122745, 2021.
- [2] F. Schedin et al., "Detection of individual gas molecules adsorbed on graphene", *Nature Materials*, vol. 6, p. 652-655, 2007.
- [3] A. Peña et al., "Optimization of multilayer graphene-based gas sensors by ultraviolet photoactivation", *Applied Surface Science*, vol. 610, p. 155393, 2023.
- [4] A. Lipatov et al., "Intrinsic device-to-device variation in graphene field-effect transistors on a Si/SiO₂ substrate as a platform for discriminative gas sensing", *Applied Physics Letters*, vol. 104, p. 013114, 2014.
- [5] S. Vollebregt et al., "A transfer-free wafer-scale CVD graphene fabrication process for MEMS/NEMS sensors", in *IEEE 29th International Conference on Micro Electro Mechanical Systems (MEMS)*, Shanghai, January 24-28, 2016, pp. 17-20.
- [6] L.N. Sacco, H. Meng, and S. Vollebregt, "Humidity sensor based on multi-layer graphene (MLG) integrated onto a micro-hotplate (MHP)", in *IEEE Sensors*, Dallas, October 30-November 2, 2022, pp. 1-4.
- [7] R. Lukose et al., "Influence of plasma treatment on SiO₂/Si and Si₃N₄/Si substrates for large-scale transfer of graphene", *Scientific Reports*, vol. 11, p. 13111, 2021.
- [8] D.R. Lenski, and M.S. Fuhrer, "Raman and optical characterization of multilayer turbostratic graphene grown via chemical vapor deposition", *Journal of Applied Physics*, vol. 110, p. 013720, 2011.
- [9] J. Romijn et al., "Multi-layer graphene pirani pressure sensors", *Nanotechnology*, vol. 32, no. 33, p. 335501, 2021.
- [10] M. Ridene, I. Iezhokin, P. Offermands, and C.F.J. Flipse, "Enhanced Sensitivity of Epitaxial Graphene to NO₂ by Water Coadsorption", *Journal of Physical Chemistry C*, vol. 120, no. 34, pp. 19107-19112, 2016.

CONTACT

*S. Vollebregt, tel: +31-15-2786788;
s.vollebregt@tudelft.nl